

$^{64}\text{Ni}(^{12}\text{C},\text{p}2\text{n}\gamma)$ **2015Ra20**

Type	Author	Citation	History Literature Cutoff Date
Full Evaluation	Balraj Singh and Jun Chen	NDS 158, 1 (2019)	16-May-2019

2015Ra20 (also [2012Ra22](#)): 55 MeV ^{12}C beam from the 15UD Pelletron at the Inter-University Accelerator Center (IUAC), New Delhi. Target=enriched, $\approx 1.5 \text{ mg/cm}^2$ thick ^{64}Ni target with a thick Au backing. The γ -rays were detected using Gamma Detector Array (GDA) consisting of 12 Compton-suppressed n-type HPGe detectors with anti-Compton shields. Measured $E\gamma$, $I\gamma$, $\gamma\gamma$ -coin, $\gamma\gamma(\theta)$ (DCO). Deduced high-spin levels, J^π , multipolarities, alignments, configurations. Results discussed in the context of triaxial particle-rotor model, cranked shell model and relativistic mean-field calculations.

 ^{73}As Levels

E(level) [†]	J^π [‡]	Comments
0.0	3/2 ⁻	
67.0 [#] 7	5/2 ⁻	
428.1 ^{&} 10	9/2 ⁺	
577.0 7	7/2 ⁻	J^π : 5/2 ⁻ in Adopted Levels.
861.0 [@] 7	7/2 ⁻	
929.2 [#] 9	9/2 ⁻	
1037.1 ^{&} 10	13/2 ⁺	
1177.9 8	9/2 ⁻	
1293.1 12	11/2 ⁺	
1657.9 [@] 8	11/2 ⁻	
1761.1 12		
1948.9 ^{&} 12	17/2 ⁺	
2039.8 [#] 9	13/2 ⁻	
2474.7 [@] 10	15/2 ⁻	
2847.7 [#] 11	17/2 ⁻	
2965.7 ^{&} 14	21/2 ⁺	
3049.9 ^a 14	19/2 ⁽⁺⁾	
3371.7 [@] 12	19/2 ⁻	
3490.1 ^b 14	21/2 ⁽⁺⁾	
3750.7 [#] 15	21/2 ⁻	
3841.7 ^c 15	19/2 ⁽⁻⁾	
4023.7 ^a 14	23/2 ⁽⁺⁾	
4082.7 ^{&} 17	25/2 ⁺	
4456.7 [@] 16	23/2 ⁻	
4586.5 ^b 14	(25/2 ⁺)	
4869.7 [#] 18	25/2 ⁻	
4963.7 ^c 18	(23/2 ⁻)	
5117.8 18		
5411.7 ^a 18	(27/2 ⁺)	
5411.8 ^{&} 20	29/2 ⁺	
5685.7 [@] 19	27/2 ⁻	
5953.5 ^b 18	(29/2 ⁺)	
6131.8 [#] 20	29/2 ⁻	
6310.8 ^c 20	(27/2 ⁻)	
6908.7 ^{&} 22	33/2 ⁺	
7433.8 [#] 23	33/2 ⁻	

Continued on next page (footnotes at end of table)

$^{64}\text{Ni}(^{12}\text{C},\text{p}2\text{n}\gamma)$ 2015Ra20 (continued) **^{73}As Levels (continued)**

E(level) [†]	J [‡]
8610.8 ^{&} 24	(37/2 ⁺)
8787.8 [#] 25	(37/2 ⁻)

[†] From least-squares fit to E γ data, assuming $\Delta E\gamma=1$ keV for each E γ .

[‡] As proposed in 2015Ra20, based on previous assignments for low-lying low-spin levels, and DCO data and band assignments for high-spin levels.

[#] Band(A): Favored band based on 5/2⁻, $\alpha=+1/2$. At low spins, configuration= $\pi(2p_{3/2}1f_{5/2}2p_{1/2})^5$. First band crossing at $\hbar\omega\approx0.45$ MeV due to pair of g_{9/2} neutrons, second possible band crossing at $\hbar\omega\approx0.6$ MeV due to pair of g_{9/2} protons; 3qp configuration after first crossing and 5qp configuration after second band crossing.

[@] Band(a): Unfavored band based on 7/2⁻, $\alpha=-1/2$. At low spins, configuration= $\pi(2p_{3/2}1f_{5/2}2p_{1/2})^5$. First band crossing at $\hbar\omega\approx0.45$ MeV due to pair of g_{9/2} neutrons, 3qp configuration after first crossing.

[&] Band(B): Band built on $\pi g_{9/2}, \alpha=+1/2$. Decoupled (favored) band. At low spins, configuration is $\pi g_{9/2}$, while at higher spins, configuration= $\pi g_{9/2} \otimes \nu g_{9/2}^2$. Unfavored partner of this band is not seen.

^a Band(C): Band based on 19/2⁽⁺⁾.

^b Band(c): Band based on 21/2⁽⁺⁾.

^c Band(D): Band based on 19/2⁽⁻⁾.

 $\gamma(^{73}\text{As})$

R_{DCO} were measured by gating on $\Delta J=2$ stretched quadrupole transitions where expected DCO ratios are ≈ 1 for stretched quadrupole transitions, and ≈ 0.5 for stretched dipole transitions.

E γ	I γ	E _i (level)	J $^\pi_i$	E _f	J $^\pi_f$	Mult.	Comments
67		67.0	5/2 ⁻	0.0	3/2 ⁻		
317	0.6 3	1177.9	9/2 ⁻	861.0	7/2 ⁻		
361		428.1	9/2 ⁺	67.0	5/2 ⁻		
373	1.8 4	2847.7	17/2 ⁻	2474.7	15/2 ⁻		
382	2.1 4	2039.8	13/2 ⁻	1657.9	11/2 ⁻		
434	3.3 9	2474.7	15/2 ⁻	2039.8	13/2 ⁻		
440	0.8 4	3490.1	21/2 ⁽⁺⁾	3049.9	19/2 ⁽⁺⁾		
468	1.2 3	1761.1		1293.1	11/2 ⁺		
480	4.2 5	1657.9	11/2 ⁻	1177.9	9/2 ⁻	(D)	DCO=0.68 14
510	5.4 9	577.0	7/2 ⁻	67.0	5/2 ⁻		
524	[†]	3371.7	19/2 ⁻	2847.7	17/2 ⁻		
526	[†]	2474.7	15/2 ⁻	1948.9	17/2 ⁺		
563	2.2 4	4586.5	(25/2 ⁺)	4023.7	23/2 ⁽⁺⁾		
577	2.5 3	577.0	7/2 ⁻	0.0	3/2 ⁻		
601	3.7 3	1177.9	9/2 ⁻	577.0	7/2 ⁻		
609	100	1037.1	13/2 ⁺	428.1	9/2 ⁺		
724	2.2 4	1761.1		1037.1	13/2 ⁺		
729	1.8 4	1657.9	11/2 ⁻	929.2	9/2 ⁻		
794	7.5 8	861.0	7/2 ⁻	67.0	5/2 ⁻	D	DCO=0.64 11
797	10.7 7	1657.9	11/2 ⁻	861.0	7/2 ⁻	Q	DCO=1.02 10
808	34.3 10	2847.7	17/2 ⁻	2039.8	13/2 ⁻	Q	DCO=1.10 9
817	14.0 12	2474.7	15/2 ⁻	1657.9	11/2 ⁻	Q	DCO=1.12 16
861	10.5 9	861.0	7/2 ⁻	0.0	3/2 ⁻	Q	DCO=1.12 11
862 [‡]	71.2 [‡] 11	929.2	9/2 ⁻	67.0	5/2 ⁻	Q	DCO=1.01 9

Continued on next page (footnotes at end of table)

$^{64}\text{Ni}(^{12}\text{C},\text{p}2\text{n}\gamma)$ **2015Ra20** (continued) $\gamma(^{73}\text{As})$ (continued)

E_γ	I_γ	$E_i(\text{level})$	J_i^π	E_f	J_f^π	Mult.	Comments
862 [‡]	2.6 [‡] 5	2039.8	13/2 ⁻	1177.9	9/2 ⁻		
865	2.1 7	1293.1	11/2 ⁺	428.1	9/2 ⁺		
897	9.6 7	3371.7	19/2 ⁻	2474.7	15/2 ⁻	Q	DCO=1.15 15
903	20.3 9	3750.7	21/2 ⁻	2847.7	17/2 ⁻	Q	DCO=1.12 7
912	78.3 9	1948.9	17/2 ⁺	1037.1	13/2 ⁺	Q	DCO=0.98 4
974	3.1 4	4023.7	23/2 ⁽⁺⁾	3049.9	19/2 ⁽⁺⁾	Q	DCO=1.13 18
994	4.5 5	3841.7	19/2 ⁽⁻⁾	2847.7	17/2 ⁻	D	DCO=0.54 21
1002	6.4 9	2039.8	13/2 ⁻	1037.1	13/2 ⁺	D	DCO=0.92 13
							Mult.: $\Delta J=0$, dipole transition.
1017	48.9 10	2965.7	21/2 ⁺	1948.9	17/2 ⁺	Q	DCO=1.05 11
1058	3.9 6	4023.7	23/2 ⁽⁺⁾	2965.7	21/2 ⁺	D	DCO=0.71 14
1085	5.9 8	4456.7	23/2 ⁻	3371.7	19/2 ⁻	Q	DCO=1.15 15
1096	3.6 5	4586.5	(25/2 ⁺)	3490.1	21/2 ⁽⁺⁾		
1101	9.2 7	3049.9	19/2 ⁽⁺⁾	1948.9	17/2 ⁺	D	DCO=0.72 13
1110	41.3 13	2039.8	13/2 ⁻	929.2	9/2 ⁻	Q	DCO=0.99 5
1111	4.6 7	1177.9	9/2 ⁻	67.0	5/2 ⁻	Q	DCO=1.17 14
1117	26.5 12	4082.7	25/2 ⁺	2965.7	21/2 ⁺	Q	DCO=0.98 10
1119	8.1 9	4869.7	25/2 ⁻	3750.7	21/2 ⁻	Q	DCO=1.10 12
1122	1.3 4	4963.7	(23/2 ⁻)	3841.7	19/2 ⁽⁻⁾		
1229	4.3 4	5685.7	27/2 ⁻	4456.7	23/2 ⁻	Q	DCO=1.15 16
1262	7.2 7	6131.8	29/2 ⁻	4869.7	25/2 ⁻	Q	DCO=1.16 17
1276	0.7 5	5117.8		3841.7	19/2 ⁽⁻⁾		
1302	4.5 6	7433.8	33/2 ⁻	6131.8	29/2 ⁻	Q	DCO=1.20 17
1329	9.7 6	5411.8	29/2 ⁺	4082.7	25/2 ⁺	Q	DCO=1.08 11
1347	1.0 5	6310.8	(27/2 ⁻)	4963.7	(23/2 ⁻)		
1354	1.5 7	8787.8	(37/2 ⁻)	7433.8	33/2 ⁻		
1367	0.9 4	5953.5	(29/2 ⁺)	4586.5	(25/2 ⁺)		
1388	0.9 5	5411.7	(27/2 ⁺)	4023.7	23/2 ⁽⁺⁾		
1438	5.9 7	2474.7	15/2 ⁻	1037.1	13/2 ⁺		DCO=1.65 19
							DCO value is inconsistent with 15/2 ⁻ to 13/2 ⁺ , dipole transition as given in Table I of 2015Ra20 . DCO is also too large for $\Delta J=2, Q$ or $\Delta J=0$, dipole. It seems consistent with $\Delta J=0$ or 1, dipole with significant quadrupole admixture.
1497	4.0 6	6908.7	33/2 ⁺	5411.8	29/2 ⁺	Q	DCO=1.17 17
1541	5.8 7	3490.1	21/2 ⁽⁺⁾	1948.9	17/2 ⁺	Q	DCO=1.21 16
1621	3.6 4	4586.5	(25/2 ⁺)	2965.7	21/2 ⁺	Q	DCO=1.17 18
1702	2.9 5	8610.8	(37/2 ⁺)	6908.7	33/2 ⁺		

[†] Intensity is not listed in Table I of [2015Ra20](#). From the width of the arrow in authors' level-scheme Fig. 1, I_γ is estimated as <2.

[‡] Multiply placed with intensity suitably divided.

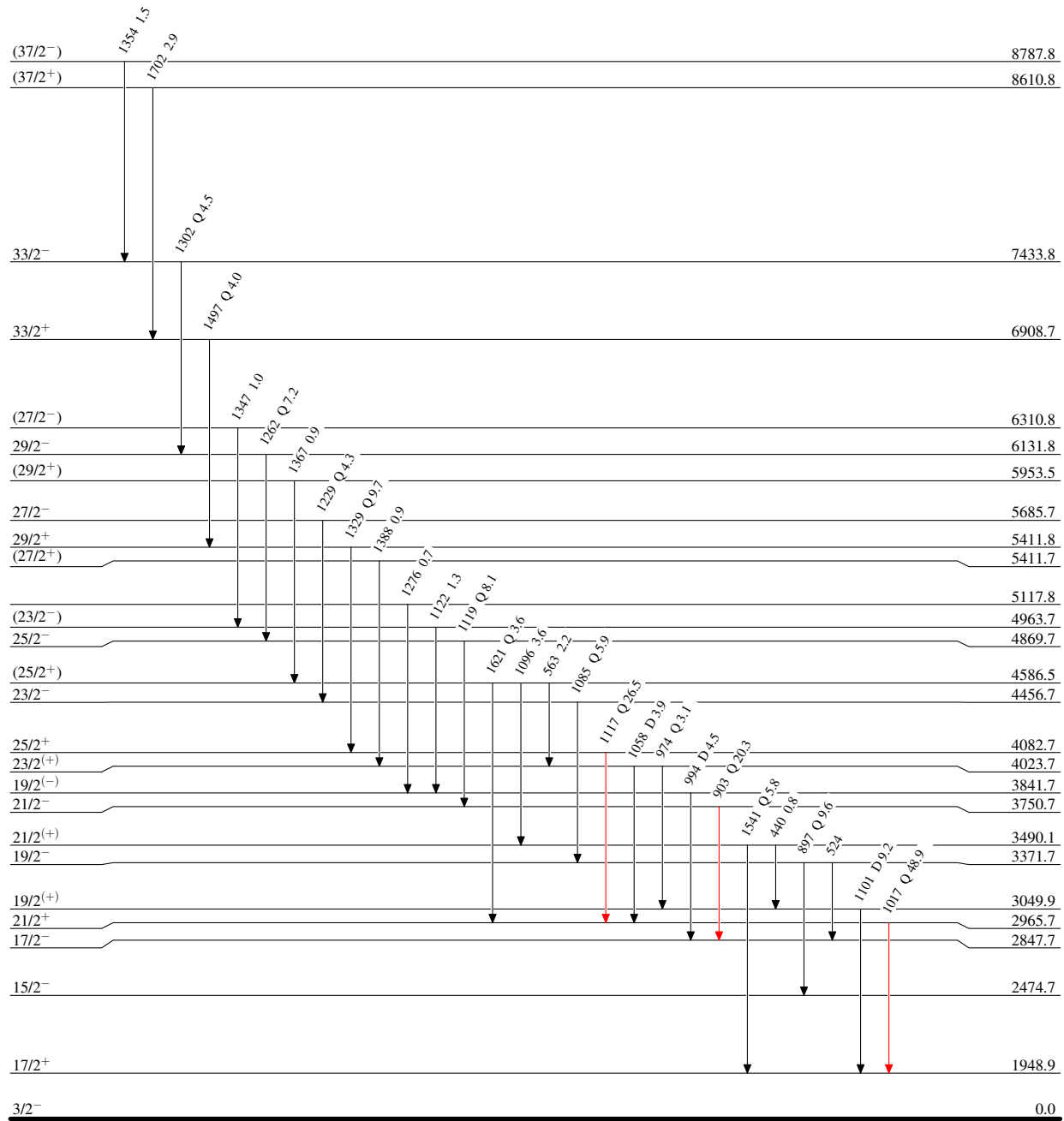
$^{64}\text{Ni}(\text{C},\text{p}2n\gamma)$ 2015Ra20

Legend

Level Scheme

Intensities: Relative I_γ

- $I_\gamma < 2\% \times I_\gamma^{\max}$
- $I_\gamma < 10\% \times I_\gamma^{\max}$
- $I_\gamma > 10\% \times I_\gamma^{\max}$



$^{64}\text{Ni}(\text{C},\text{p}2n\gamma)$ 2015Ra20

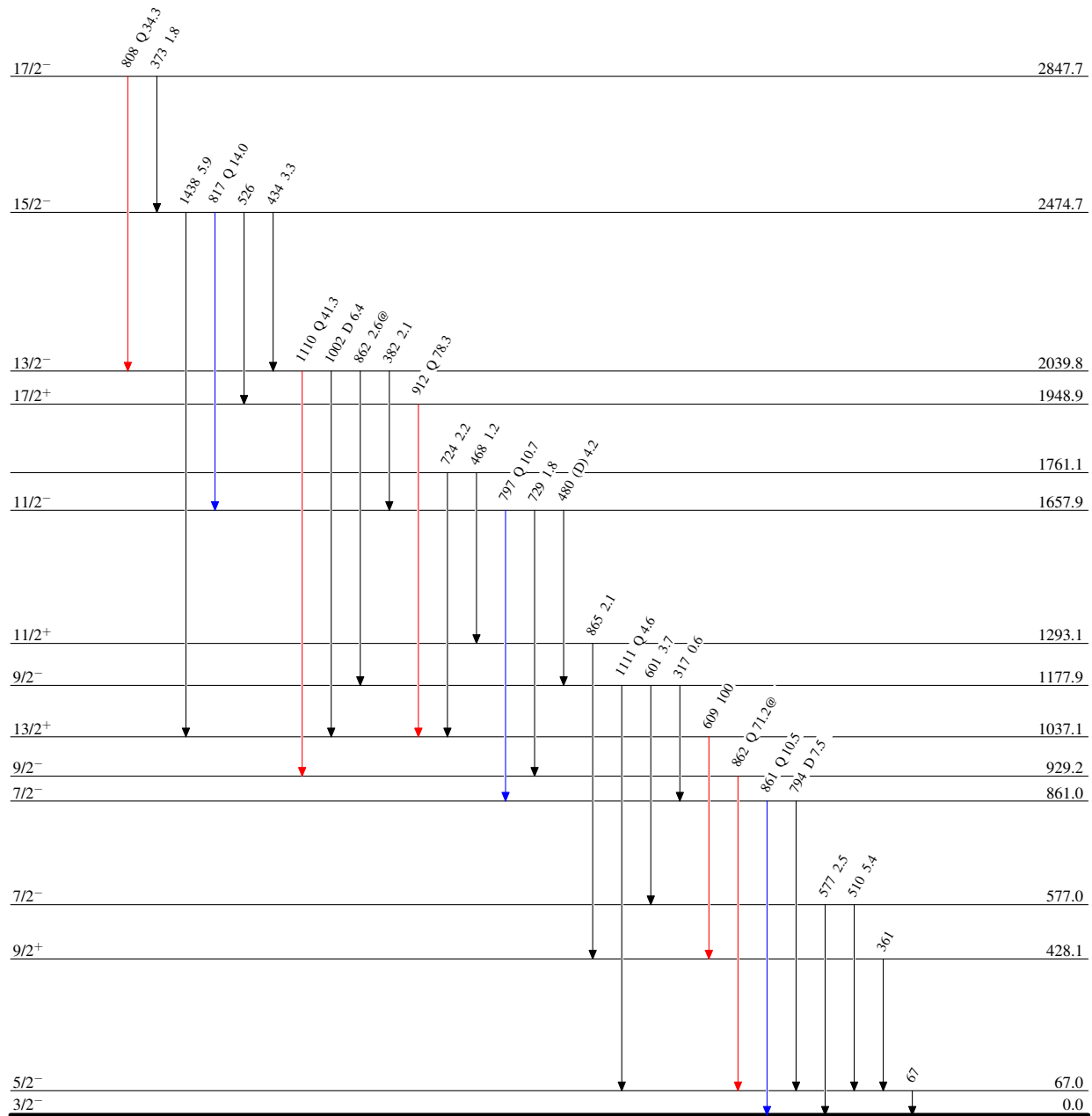
Level Scheme (continued)

Intensities: Relative I_γ

@ Multiply placed: intensity suitably divided

Legend

- $I_\gamma < 2\% \times I_{\gamma}^{\max}$
- $I_\gamma < 10\% \times I_{\gamma}^{\max}$
- $I_\gamma > 10\% \times I_{\gamma}^{\max}$



$^{64}\text{Ni}(\text{C},\text{p}2\text{n}\gamma)$ 2015Ra20